Dynamical diffraction explanation of the anomalous transmission of light through metallic gratings

M. M. J. Treacy
NEC Research Institute, Inc., 4 Independence Way, Princeton, New Jersey 08540-6685
(Received 25 February 2002; revised manuscript received 13 June 2002; published 13 November 2002)

In this paper, it is pointed out that the light transmission anomalies observed for thin-film metallic gratings can be explained entirely in terms of dynamical diffraction theory. Surface plasmons are an intrinsic component of the diffracted wave field and, as such, play no independent causal role in the anomalies, as has been implied by others. The dynamical scattering matrix for the Bloch-wave modes of the diffracted photon wave field (**E**, **H**) is derived for a three-dimensionally periodic medium with arbitrary dielectric constant. A new theoretical treatment and numerical results are presented for a one-dimensional array of slits. In model metallic slit arrays, with negative dielectric constant, 100% and 0% transmission is possible at different wavelengths in the zero-order beam. In slit arrays, both propagating and evanescent modes (traditional surface plasmons) are strongly excited at both the peak and the minimum transmission conditions.

DOI: 10.1103/PhysRevB.66.195105 PACS number(s): 41.20.Jb, 42.79.Dj

I. INTRODUCTION

Ebbesen and colleagues[1,2] have reported that a periodic thin-film metallic grating, formed from a two-dimensional array of holes, can transmit more light at certain wavelengths than the projected area of the holes in the grating would suggest. At other wavelengths, transmission is almost fully blocked. The enhancement in the transmitted zero-order beam is reported to be several orders of magnitude larger than that from an isolated subwavelength aperture, after normalizing for the relative hole area.[1,3] This discovery has sparked much interest in the possibility of fabricating efficient transmissive photonic structures, such as subwavelength scanning probes.

The strong ''anomalous'' transmissions and extinctions that occur when x rays are diffracted by crystals are now well understood in terms of Ewald's 90-year-old dynamical diffraction theory.[4,5] The physics governing the scattering of light (both propagating and evanescent modes) by periodic metallic gratings at optical wavelengths is *formally identical* to that governing the coherent dynamical diffraction of x rays by crystals. The different scattering properties of the periodic dielectric media are entirely encapsulated in the spatial variation of the complex dielectric permittivity, whose real part can be large and negative in metals and close to unity for x rays in crystals. It would seem reasonable to claim that the anomalous transmission of light observed in thin metallic hole arrays shares a common physical origin with the transmission anomalies observed in x-ray diffraction.

To date, three physical models have been proposed to explain transmission anomalies in hole arrays. The first argues that it is simply a dynamical diffraction resonance in a periodic material with a substantially negative ($\epsilon < -1$) dielectric constant.[6] This is the viewpoint of this paper. The second proposes that transmission is caused by surface plasmons whose resonances are enhanced by the metallic hole array.[1,2,7–16] A third interpretation, specific to one-dimensional gratings, treats the slits as open Fabry-Pérot resonant cavities,[8,17–19] which act as efficient waveguides. Judging from the published literature to date, most researchers in this area favor a causal surface plasmon explanation, while acknowledging that diffraction plays an important negative role in the transmission dips—the so-called Wood-Rayleigh anomalies.[20,21] Recently, Cao and Lalanne[19] have argued that in fact it is the surface plasmons that are most strongly excited near the Wood-Rayleigh anomalies and are most weakly excited at the transmission maxima, a point that had been previously admitted by some proponents of the surface plasmon explanation.[8] Cao and Lalanne[19] went further and argued that it is the surface plasmons that play a negative role in the transmission anomalies in slit arrays and that it is a combination of strongly excited waveguide and diffraction modes that lead to transmission enhancement in slit arrays. Although it is clear that all the proposed models are implicitly incorporating elements of each other in the physics, they all produce essentially identical predictions for arrays of slits, the emphasis in each model resting on different photon scattering modes and on the language describing the scattering. Consequently, there is not yet a consensus on the physical mechanism causing the transmission anomalies.

Supporters of a coherent dynamical diffraction explanation argue that since the experiment involves the diffraction of light from a thin metallic diffraction grating and then measuring the intensity in the zero-order transmitted diffracted beam, diffraction is obviously playing an important role.[6] The evanescent diffraction modes are related to the surface plasmons, which are therefore implicitly included but, along with any propagating ''Bragg-reflected'' beams, are not assigned any causal properties. In addition, initial reports appeared to overlook the inherent coherence of the light emerging from each aperture. If we treat each aperture at the exit surface as a point source, then the light emerging from each is a spherical wave with equal amplitude transmitted in all directions. For N-point sources, periodic or otherwise, the enhancement of the energy density in the zero-order mode (measured by a point detector in the far-field) is expected to scale as N^2, not N, because of constructive interference. This does not violate energy conservation because the far field energy density for most other $g \neq 0$ directions is diminished by destructive interference. If $\lambda < d$, where d is the array spacing, additional beams of high-energy density will appear,

corresponding to diffraction orders, or Bragg beams. Only for a collection solid angle of 2π is the linear dependence on N strictly applicable. Compensating for this coherent, nondynamical, diffraction effect, the residual enhancement due to the grating alone appears to be around 3 or 4.

A further compelling argument in favor of a dynamical diffraction explanation comes from the well-known fact that similar strong transmission anomalies are observed in transmission electron microscopy[22] and x-ray topographic[23] studies of crystals. Pendellösung (or thickness) fringes, as well as bend contours, are due to strong fluctuations in the transmitted intensity caused by dynamical diffraction effects. Similar fluctuations would be expected when the wavelength of the electrons and x-ray photons are varied, although the wavelength is not usually a variable in those experiments. Further, the wave equations governing the scattering of light in hole arrays are formally identical to those governing the diffraction of x rays in crystals. The principal differences are in the material details; the metal in hole arrays has a dielectric constant that is large and negative (as opposed to being slightly larger than unity for x-ray scattering in crystals), and the periodicities and wavelengths are 3–4 orders of magnitude larger (microns, compared with angstroms in typical crystals). Because of the weak scattering of x rays in crystals, a significant simplification can be made for thin crystals which leads to the kinematical (single-scattering event) diffraction theory. An equivalent simplification cannot be made for the strong dynamical scattering occurring in metallic hole arrays or optical band-gap materials.

Proponents of the resonant cavity model point out that there is a propagating TM waveguide mode in one-dimensional (1D) slit arrays and that the cavity has an effective index of refraction that is greater than unity, even though the cavity may be empty. An elegantly simple model, based on resonant cavities,[17–19] matches remarkably well the results of a full electromagnetic simulation using a rigorous coupled-wave analysis (RCWA).[24–26] However, it is known that 2D arrays of subwavelength open cylinders do not support propagating waveguide modes.[27]

Advocates of the surface plasmon model note that light is known to couple to surface plasmon modes on metals.[28] In favor of a causal role for surface plasmons, some researchers[29] point out that the most pronounced transmission anomalies occur in metals, such as silver, which are known to support strong surface plasmon resonances. Hole arrays in materials such as germanium, which do not support strong surface plasmon resonances, do not exhibit strong transmission anomalies. In addition, when a grating made from a metal that supports relatively weak transmission anomalies, such as nickel, is coated with a relatively thin layer of silver on the top and bottom surfaces, the transmission anomalies increase significantly.[12] Since only the surfaces were modified, it is reasoned that surface plasmons must be responsible. It has been proposed that surface plasmons can squeeze light into subwavelength holes because the photon can hop and tunnel resonantly between ''plasmon molecules.''[14] Although coherent diffraction is inherently present in the physical models that underpin these claims, since the models are based on Maxwell's wave equations in periodic media, some interpretations seem to suggest that the surface plasmons pre-exist on the gratings independently of the scattering. Proponents of surface plasmons have so far failed to clearly identify the resonance mechanism responsible for generating these modes—that is, coherent diffraction. There has been a tendency to reify surface plasmons by implying that they somehow *cause* the transmission anomalies, having the power to transmit and focus light,[14] even though they are an integral part of the coherently diffracted wave field.

It has been argued[1,2,29] that diffraction cannot be playing a role in the transmission enhancements for a number of reasons, which include the following. (1) The wavelengths λ at which the most pronounced transmission anomalies occur are larger than the hole spacings d. No diffracted beams can be excited at the condition $\lambda > d$, and indeed no first-order diffracted beams emerge from the gratings. (2) Light cannot possibly be ''squeezed'' by any diffraction mechanism into such small holes, whose width is significantly less than the photon wavelength. (3) Diffraction requires propagating modes to occur in the grating. Since the skin depth in metals is significantly shorter than the grating thickness t and the hole spacing d, no significant electric fields are permitted in the grating metal. It is reasoned that all diffraction modes must therefore be strongly attenuated in the grating. Diffraction, it is claimed, is responsible only for the dips in transmission at the Wood-Rayleigh anomalies, which correspond to conditions where higher-order Bragg beams emerge at angles close to 90° to the grating normal.

These arguments highlight the fact that the kinematical (single-scattering) diffraction view, where a simple set of propagating plane waves (Bragg beams) are excited, is insufficient to explain these anomalies. As is shown here, these objections are overcome in the dynamical diffraction view, in which diffracted modes are generated by, and continuously coupled through, the periodicities in the grating. In this view, the transmitted beam is the zero-order diffracted beam—it is not an unscattered beam. Thus a propagating diffracted beam *does* emerge from the sample, and in fact this is the mode that was measured in the early experiments reporting the transmission anomalies. Evanescent diffraction modes also exist in the vicinity of the surfaces. These nonpropagating diffraction modes are associated with traditional surface plasmons and tend to decay away from the grating surfaces. Further, and most importantly, the absence of higher-order propagating diffraction modes emerging in air does not mean the absence of higher order propagating modes inside the grating. The coupling of diffraction orders can be viewed in terms of Bloch waves, where each Bloch-wave mode j has an effective refractive index $n^{(j)}$ associated with it. The real part of $n^{(j)}$ can be large and positive for some modes, yielding an effective wavelength $\lambda/n^{(j)}$ in the grating that is less than the hole spacing. Thus, at normal incidence, propagating modes can occur in the grating that satisfy $\lambda < n^{(j)}d$. TM-polarized propagating Bloch waves in arrays of slits have their electric-field amplitude concentrated over the holes. The existence of such modes does not necessarily imply strong electric fields in the metal. Such propagating Bloch waves can be viewed as guided waves in a medium with an effective dielectric

constant that is larger than unity, consistent with the view of Lalanne and others.[17–19]

The view that the Wood-Rayleigh anomalies are caused by the creation and annihilation of higher-order Bragg beams at 90° (i.e., diffraction causes transmission extinctions[1,2]) seems to overlook the logically complementary (and equally simplistic) view that the Wood-Rayleigh anomalies are caused by the annihilation and creation of resonant surface plasmon modes with long attenuation lengths; i.e., surface plasmons are the cause of the extinctions. A better way to view the Wood-Rayleigh anomalies is that they arise when the real part of a Bloch-wave propagation wave vector vanishes, defining a transition between being a propagating (possibly attenuated) Bloch-wave mode to a purely evanescent Bloch-wave mode.

It has been shown that, while slit arrays can support efficient TM waveguide modes, two-dimensional hole arrays are a different matter.[27] Attenuated TE polarization states inevitably occur in this geometry. Consequently two-dimensional hole arrays cannot be viewed as an array of efficient cylindrical waveguides. However, this result does not mitigate against the role of coherent dynamical diffraction, which handles both propagating and evanescent modes seamlessly.

In this paper, a more detailed explanation is presented as to how the transmission enhancements in metallic hole arrays can be explained *entirely* as a coherent dynamical diffraction phenomenon in a modulated metallic medium, with no reified role for surface plasmons necessary. Surface plasmons are indeed excited and are an intrinsic part of the diffracted wave field. Numerical results are presented for one-dimensional slit arrays, a geometry that allows the dynamical equations to be solved in a novel manner, as a straightforward eigenvalue problem.[6] This geometry has also been solved by proponents of the surface plasmon[8] and waveguide[19] viewpoints, with similar results, confirming the validity of the dynamical diffraction approach. It is shown that propagating Bloch-wave modes, equivalent to waveguide modes with electric field confined to the cavities, can be strongly excited in slit arrays. It is shown how the surface plasmon charge density can be obtained directly from the coherently diffracted wave field $\mathbf{E}(\mathbf{r})$. It is concluded that elements of the surface plasmon and waveguide viewpoints are inherently present in the dynamical diffraction interpretation.

II. THEORY

A. Coherent diffraction in periodic media

When a plane wave of light impinges on a small particle, some of the incident light is scattered sideways and backwards. This is true whether the object be transparent, opaque, or reflecting, although these properties influence the phase and amplitude of the scattering. When the particle is much smaller than the wavelength of light, becoming essentially a point, the scattered wave resembles a spherical wave. In the Huyghens-Fresnel view of light propagation,[30] a continuous medium can be considered to be a compact, aperiodic, assembly of such small scatterers. A wave front impinging an a layer of these scatterers is transformed into a myriad of coherent spherical waves, which mutually interfere to generate the scattered wave front, which subsequently impinges on the next layer, and so on. This approach works well for modeling the scattering of light from objects of arbitrary shape and scattering properties, and reveals the underlying diffractive nature of light scattering.

In a homogeneous medium, each point scatters light identically, with the result that, statistically, the scattered light experiences destructive interference in all directions except forwards, backwards, and in the specular reflection direction. The wavelength of the light in the medium is modified by a refractive index n to λ/n. Here n may be complex, indicating absorption or reflection. When the medium possesses a macroscopic periodicity, constructive interferences can occur in additional directions. A plane wave front becomes deformed by the evolution of a set of spatial modes *whose Fourier components are those of the structure*. Not all modes are propagating, and many can be evanescent along the nominal propagation direction of the wave front. These diffraction modes are strongly resonant in a periodic structure because they have a phase $\mathbf{g}\cdot\mathbf{r}=2n\pi$ relative to the forward scattered (integer $n=0$) beam. $\mathbf{g}$ is the diffraction wave vector, which is related to the structure's periodicities of wavelength $\lambda_{x,y,z}$ via $\mathbf{g}=2\pi(n_x/\lambda_x, n_y/\lambda_y, n_z/\lambda_z)$, where the $n_{x,y,z}$ are integers. Constructive interference between beams scattered by similar points in the grating is assured by the spatial coherence of the incident wave front, and no superluminal communication between scatterers is required to provide this coherence. This resonance phenomenon lies at the heart of diffraction in periodic media. Diffraction occurs whether the periodic material be transparent, absorbing, reflecting, or magnetic. These physical properties are embodied in the dielectric constant ϵ and the magnetic permittivity μ of the material and strongly influence the amplitude, phase, and effective wave vector of the diffracted modes. Thus, different materials scatter differently into these spatial modes. In principle, a complete description of the scattering from the object can be obtained using Maxwell's equations if ϵ, μ, and the shape of the object are known.

B. Bloch-wave dynamical scattering model for the diffracted wave field in hole arrays

It is well known that Maxwell's wave equations can be solved in periodic media by expressing the solutions as a linear sum of plane-wave states, with Fourier components matching those of the medium. Ewald demonstrated this with his dynamical diffraction theory of x-ray scattering in crystals.[4] Much later, other models, such as the rigorous coupled-wave analysis for metallic surface-relief gratings, have been introduced[24] and improved for the case of transmission gratings.[25,26,31,32] Meade and co-workers[33,34] have formulated a variant of the dynamical diffraction theory for optical band-gap materials.

Here the dynamical diffraction problem is solved in terms of Bloch-wave modes, analogously to the method of Ewald, but valid for a periodic medium with arbitrary dielectric constant. In the case of x-ray diffraction in crystals, the scattering is sufficiently weak that the effective value of $\epsilon(\mathbf{r})$ devi-

ates only slightly from unity. This allows a significant simplification of the wave equations for x-ray scattering. Further, the three-dimensional periodicity of crystals simplifies matters so that only those propagating Fourier components that lie close to the Ewald sphere need to be considered. Since the Fourier components of the dielectric constant for x rays in crystals tend to be much less than unity, the deformations and branchings that open up on the Ewald sphere tend to be small perturbations, allowing easy determination, in advance of any computation, of the likely strongly excited Fourier components. In metallic hole arrays and optical band-gap materials, ϵ can be large (the real parts of ϵ tend to be large and negative in the former and large and positive in the latter), and the simpler eigenvalue equations derived for the weaker x-ray scattering are not appropriate. The streaky nature of the Fourier coefficients perpendicular to the grating normal means that many modes can intersect the Ewald sphere that are not near a true Bragg condition. Additionally, the strongly dynamical (multiple-scattering) nature of the diffraction ensures that many modes can be simultaneously excited, including those that do not directly intersect the Ewald sphere; thus the important strongly excited modes are not easily guessed in advance.

For an inhomogeneous nonferroelectric medium, the wave equations governing the electric, **E**, and magnetic, **H**, fields are obtained directly from Maxwell's equations:

$$\boldsymbol{\nabla}\times\left[\frac{1}{\mu(\mathbf{r})}\boldsymbol{\nabla}\times\mathbf{E}(\mathbf{r})\right]-\chi^2\epsilon(\mathbf{r})\mathbf{E}(\mathbf{r})=0, \tag{1}$$

$$\boldsymbol{\nabla}\times\left[\frac{1}{\epsilon(\mathbf{r})}\boldsymbol{\nabla}\times\mathbf{H}(\mathbf{r})\right]-\chi^2\mu(\mathbf{r})\mathbf{H}(\mathbf{r})=0. \tag{2}$$

As usual, ε is the dielectric constant, and μ is the magnetic permeability, which, in general, may be large and complex. $\boldsymbol{\chi}$ is the vacuum wave vector of the plane wave incident on the grating and, for wavelength λ, has amplitude $2\pi/\lambda$.

For a nonmagnetic grating $\mu(\mathbf{r})=1$ everywhere, Eq. (1) reduces to

$$\boldsymbol{\nabla}\times\boldsymbol{\nabla}\times\mathbf{E}(\mathbf{r})-\chi^2\epsilon(\mathbf{r})\mathbf{E}(\mathbf{r})=0. \tag{3}$$

Since we wish to solve these equations for a general polarization, Eq. (2) is considerably more congenial to the task than is Eq. (3). This is because $\mu(\mathbf{r})$ being constant ensures that the magnetic field $\mathbf{H}(\mathbf{r})$ is orthogonal to the propagation direction.

The grating is illuminated by an incident plane wave $[H_1^{\mathrm{inc}}\hat{\mathbf{n}}_1+H_2^{\mathrm{inc}}\hat{\mathbf{n}}_2]\exp(i\boldsymbol{\chi}\cdot\mathbf{r})$. Here H_1^{inc} is the amplitude of the incident magnetic field polarization parallel to the unit vector $\hat{\mathbf{n}}_1$, and similarly, H_2^{inc} is the polarization component of the incident magnetic field parallel to the unit vector $\hat{\mathbf{n}}_2$. Here $\hat{\mathbf{n}}_1$ and $\hat{\mathbf{n}}_2$ are chosen such that $\hat{\mathbf{n}}_1$, $\hat{\mathbf{n}}_2$, and $\boldsymbol{\chi}$ are mutually perpendicular.

The grating is periodic, so we can represent the reciprocal of the complex dielectric constant, $\epsilon(\mathbf{r})^{-1}$, the dielectric restriction, as

$$\epsilon(\mathbf{r})^{-1}=\sum_g F_g\exp(i\mathbf{g}\cdot\mathbf{r}). \tag{4}$$

where the **g** are the Fourier harmonics of the grating periodicity. The coefficients F_g are generally complex.

We look for Bloch-wave solutions for the scattered wave field inside the periodic grating. Such solutions can be represented by the sum of polarized plane-wave states:

$$\mathbf{H}^{(j)}(\mathbf{r})=\sum_g\sum_p\hat{\mathbf{n}}_{p,g}^{(j)}H_{p,g}^{(j)}\exp[i(\mathbf{k}^{(j)}+\mathbf{g})\cdot\mathbf{r}]. \tag{5}$$

For the jth Bloch wave, the $H_{p,g}^{(j)}$ have no **r** dependence. The $\hat{\mathbf{n}}_{p,g}^{(j)}$ $(p=1,2)$ are two unit vectors associated with each plane wave $\mathbf{k}^{(j)}+\mathbf{g}$. The direction of each unit vector is fixed by the choice of Cartesian axes and from Maxwell's equations—that is,

$$\begin{aligned}\boldsymbol{\nabla}\cdot\mathbf{H}^{(j)}(\mathbf{r})&=\boldsymbol{\nabla}\cdot\sum_g\sum_p\hat{\mathbf{n}}_{p,g}^{(j)}H_{p,g}\exp[i(\mathbf{k}^{(j)}+\mathbf{g})\cdot\mathbf{r}]\\&=i\sum_g\sum_p(\mathbf{k}^{(j)}+\mathbf{g})\cdot\hat{\mathbf{n}}_{p,g}^{(j)}H_{p,g}^{(j)}\exp[i(\mathbf{k}^{(j)}+\mathbf{g})\cdot\mathbf{r}]\\&=0;\end{aligned} \tag{6}$$

thus, in general, we assert

$$(\mathbf{k}^{(j)}+\mathbf{g})\cdot\hat{\mathbf{n}}_{p,g}^{(j)}=0. \tag{7}$$

This ensures that the magnetic field of each plane-wave state is transverse to the direction of propagation. Furthermore, to ensure that the two field components are mutually independent, we assert the orthogonality requirement

$$\hat{\mathbf{n}}_{1,g}^{(j)}\cdot\hat{\mathbf{n}}_{2,g}^{(j)}=0. \tag{8}$$

The total magnetic field is given by the sum of each Bloch-wave excitation for both polarizations:

$$\mathbf{H}(\mathbf{r})=\sum_j\psi_p^{(j)}\sum_g\sum_p\hat{\mathbf{n}}_{p,g}^{(j)}H_{p,g}^{(j)}\exp[i(\mathbf{k}^{(j)}+\mathbf{g})\cdot\mathbf{r}], \tag{9}$$

where $\psi_p^{(j)}$ is the excitation of the p-polarized Bloch wave j. The total electric field $\mathbf{E}(\mathbf{r})$ is then found from Maxwell's equations:

$$\begin{aligned}\mathbf{E}(\mathbf{r})&=-\frac{1}{i\omega\epsilon_0}\frac{1}{\epsilon(\mathbf{r})}\boldsymbol{\nabla}\times\mathbf{H}(\mathbf{r})\\&=-\frac{1}{\omega\epsilon_0}\sum_h F_h\sum_j\psi_p^{(j)}\sum_g\sum_p(\mathbf{k}^{(j)}+\mathbf{g}-\mathbf{h})\\&\quad\times\hat{\mathbf{n}}_{p,g-h}^{(j)}H_{p,g-h}^{(j)}\exp[i(\mathbf{k}^{(j)}+\mathbf{g})\cdot\mathbf{r}].\end{aligned} \tag{10}$$

In the absence of free charges, the polarization charge density is $\rho=\boldsymbol{\nabla}\cdot\mathbf{P}=-\epsilon_0\boldsymbol{\nabla}\cdot\mathbf{E}$. Thus, for the $p=1$ polarization (TM polarization, **H** parallel to slits)

$$\rho(\mathbf{r}) = -\frac{i}{\omega}\sum_j \psi_1^{(j)} k_z^{(j)} \sum_g \sum_h hF_h H_{1,g-h}^{(j)} \exp[i(\mathbf{k}^{(j)}+\mathbf{g})\cdot\mathbf{r}] \tag{11}$$

and for $p=2$ (TE polarization, **E** parallel to the slits)

$$\rho(\mathbf{r}) = 0. \tag{12}$$

$k_z^{(j)}$ is the z component of the wave vector $\mathbf{k}^{(j)}$.

Each Bloch wave is independently a solution to Maxwell's equations. We take the Fourier transform of Eq. (2):

$$\int e^{-i\mathbf{k}'\cdot\mathbf{r}} \left\{ \nabla \times \left[\frac{1}{\epsilon(\mathbf{r})} \nabla \times \right] - \chi^2 \right\} \mathbf{H}^{(j)}(\mathbf{r}) d\mathbf{r} = 0. \tag{13}$$

Substituting for $\epsilon(\mathbf{r})^{-1}$ from Eq. (4) and for $\mathbf{H}^{(j)}(\mathbf{r})$ from Eq. (5), after some manipulation we get for each polarization state $p=1,2$ the equation

$$\sum_h F_{g-h}[(\mathbf{k}^{(j)}+\mathbf{g})\times\hat{\mathbf{n}}_{p,g}^{(j)}]\cdot[(\mathbf{k}^{(j)}+\mathbf{h})\times\hat{\mathbf{n}}_{p,h}^{(j)}] H_{p,h}^{(j)} - \chi^2 H_{p,g}^{(j)} = 0. \tag{14}$$

This eigenvalue equation is a generalized form of the dynamical scattering matrix originally derived by Ewald[4,5] to describe diffraction of x rays by crystals. This equation also closely resembles that presented by Meade and co-workers[33,34] for their treatment of optical band-gap materials. The principal difference is that in their treatment, the Bloch-wave frequencies $\omega^{(j)}$ (i.e., energies) are the eigenvalues when $\mathbf{k}$ is given. Here, ω is fixed and the $\mathbf{k}^{(j)}$ are the eigenvalues.

The eigenvalues $\mathbf{k}^{(j)}$ of Eq. (14) are generally complex, being equal to $(k_x^{(j)}, k_y^{(j)}, k_z^{(j)} + ik'^{(j)}_z)$. Typically, $k_x^{(j)}$ and $k_y^{(j)}$ are given by the experimental geometry and are the same for all eigenvectors. We thus drop the superscript and refer only to k_x and k_y. We wish to solve for $k_z^{(j)}$ to obtain the dispersion surface, which is a plot of $k_z^{(j)}$ versus k_x over the Brillouin zone. $k'^{(j)}_z$ gives the attenuation of each Bloch wave along z.

Equation (14) is a general eigenvalue problem, and the elegant energy-minimizing numerical methods used by Meade and co-workers[33,34] for finding the real frequency eigenvalues ω do not apply directly to the complex wave vector $k_z^{(j)} + ik'^{(j)}_z$ eigenvalue problem. However, for the case of a one-dimensional array of slits, periodic along x, a useful simplification can be made for the $p=1$ TM polarization state, where the **H** polarization is parallel to the slits. The vector term simplifies to

$$\begin{aligned}[(\mathbf{k}^{(j)}+\mathbf{g})\times\hat{\mathbf{n}}_{p,g}^{(j)}]\cdot[(\mathbf{k}^{(j)}+\mathbf{h})\times\hat{\mathbf{n}}_{p,h}^{(j)}] &= (\mathbf{k}^{(j)}+\mathbf{g})\cdot(\mathbf{k}^{(j)}+\mathbf{h}) \\ &= (k_x+g,0,k_z^{(j)})\cdot(k_x+h,0,k_z^{(j)}) \\ &= (k_x+g)(k_x+h)+k_z^{(j)\,2}. \end{aligned} \tag{15}$$

Thus, for the TM polarization state $p=1$, we have

$$\sum_h F_{g-h}(k_x+g)(k_x+h)H_{1,h}^{(j)} + k_z^{(j)\,2}\sum_h F_{g-h}H_{1,h}^{(j)} - \chi^2 H_{1,g}^{(j)} = 0. \tag{16}$$

This matrix equation takes the form

$$\mathbf{A}\cdot\mathbf{H} = (k_z^{(j)})^2 \mathbf{C}\cdot\mathbf{H} \tag{17}$$

or

$$(\mathbf{C}^{-1}\mathbf{A})\cdot\mathbf{H} = (k_z^{(j)})^2\mathbf{H}, \tag{18}$$

where the matrix elements are

$$A_{gh} = F_{g-h}(k_x+g)(k_x+h) - \chi^2\delta_{gh} \tag{19}$$

and

$$C_{gh} = -F_{g-h}. \tag{20}$$

These matrices are not Hermitian since, in general, $F_{g-h} \neq F_{h-g}^*$ unless $\epsilon(\mathbf{r})$ is real everywhere. Consequently, the eigenvalues $(k_z^{(j)})^2$ are expected to be complex. Equation (18) represents a new and straightforward mathematical model for solving the one-dimensional grating problem. However, the harder-to-solve general form, Eq. (14), is a fully three-dimensional treatment, valid provided the medium is of large width and the thickness of the medium is an integral number of unit cells. This latter proviso arises because of the underlying assumption of periodic continuation.

The perpendicular TE polarization mode $p=2$ can be solved similarly by solving the equivalent equation for the **E** form of the Bloch waves, obtained in a similar manner starting from Eq. (3).

We can determine the excitation of each Bloch wave by satisfying boundary conditions for both the electric and magnetic fields at the upper and lower surfaces of the grating. Since we have set $\mu=1$ everywhere, then both $H_\parallel$ and $H_\perp$ are continuous across each interface. The electric field must be such that there is continuity of $E_\parallel$ and $\epsilon E_\perp$ across each interface. Finally, since we are not including any energy loss mechanisms, energy is conserved. Thus, the total scattered energy, both reflected and transmitted through the other side, must equal the incident energy.

There are two boundaries and four distinct wave fields to consider. Wave field 1 includes the incident wave, the reflected wave, and back-diffracted waves. Wave field 2 includes the (nominally) forward-propagating waves in the grating.[35] Wave field 3 is the set of back-propagating waves inside the grating, and wave field 4 contains the transmitted beams in the medium on the other side of the grating. The four sets of boundary condition equations that are obtained are similar in form to those presented by Maharam and Gaylord[24] and so are not repeated here.

Generalized eigenvalue problems of the type presented by Eq. (18) are readily solved numerically by standard eigenvalue packages, such as the LAPACK subroutine ZGEEVX.[36]

The number of Fourier components required to reach a stable solution can be quite large. For the most part, modes out to $\pm 25G$ (51 Fourier modes in total) are sufficient for most wavelengths and grating thicknesses. However, at cer-

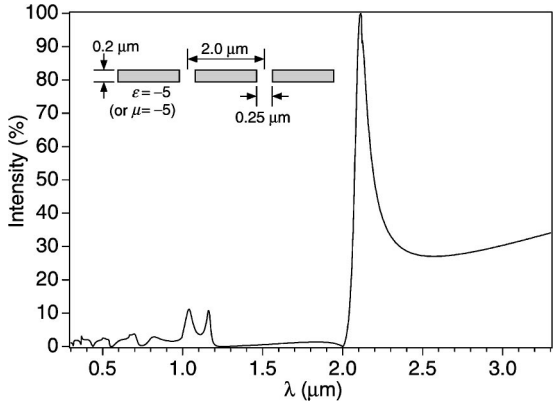

FIG. 1. Transmitted intensity vs photon wavelength for a free-standing one-dimensional grating with period 2.0 μm, slit width 0.25 μm, and thickness 0.2 μm. The grating material is modeled with $\epsilon=-5$ and $\mu=1$ for all wavelengths. $\pm 100G$ Fourier components were included. The **H**-field polarization is off the page (TM polarization). There is almost 100% transmission at $\lambda=2.117$ μm. The identical transmission spectrum is obtained for a grating material with $\epsilon=1$ and $\mu=-5$ for all wavelengths. In this latter case the **E**-field polarization vector is off the page.

tain combinations of wavelength and thickness, strong spurious resonances appear. At these conditions, modes out to $\pm 100G$ (201 Fourier modes in total) are then required for thicknesses up to 1 μm in silver. It has been found that, for the RCWA formulation of the problem, substituting the dielectric restriction matrix $\mathbf{F}\equiv\|1/\epsilon\|$ with $\|\epsilon\|^{-1}$ can produce a dramatic speedup in convergence rate in electromagnetic problems of the type considered here.[25,26,32,37] This result is all the more remarkable when it is realized that the substituted Fourier coefficients themselves converge much more slowly to the target dielectric function. It appears that the improved convergence rate arises because the substitution improves the stability of the boundary value matrix—the instability coming from the fact that the equations contain products of discontinuous Fourier series.[37] This substitution was not implemented in this work, but will clearly provide improved numerical convergence rates when addressing the two-dimensional hole array problem.

III. NUMERICAL SIMULATIONS

Figure 1 shows a simulation of the intensity in the transmitted beam I_0 as a function of the TM-polarized incident photon wavelength for an ideal one-dimensional metallic grating. The grating has a periodicity of 2.0 μm, a slit width of 0.25 μm, and a thickness of 0.2 μm. The dielectric constant is set to $\epsilon=-5$ at all wavelengths, and $k_x=0$ for normal incidence. The simulation was performed for $\pm 100g$, Fourier components, for a total of 201 Fourier components. The plot for 161 Fourier components was not substantially different, suggesting that reasonable numerical convergence has been reached.

A striking feature of this plot is that the transmitted intensity in this idealized metal is 100% at a wavelength of $\lambda=2.117$ μm. This peak occurs at a wavelength that is larger than the periodicity, $\lambda>d$, where no high-order propagating modes are supported in air (where we assume $\epsilon=1$).

Dynamical diffraction simulations of I_0 versus λ for slits in a real metal, such as silver, reproduce well the essential features of the data[6] and concur with simulations made by surface plasmon advocates.[8]

Not all of the modes inside the grating at this $\lambda>d$ condition are evanescent. Figure 2 shows Bloch-wave dispersion surfaces, computed for $\pm 25G$ Fourier components, for a total of 51 Fourier components, at four photon wavelengths $\lambda=0.8$, 1.9, 2.117, and 10.0 μm, respectively. Again, the dielectric constant is set to $\epsilon=-5$ at all wavelengths. These dispersion surfaces are plots of k_z versus k_x for each Bloch-wave branch and are plotted out to the Brillouin zone boundary, beyond which they are periodically continued. For each wavelength, the real parts of k_z associated with the propagating (pure real) and attenuated (mixed real and imaginary) modes are plotted on the left. The complex components of k_z associated with the attenuated and evanescent (pure complex) modes are plotted on the right. In a real metal, such as silver, the propagating Bloch wave vectors generally have both real and imaginary components and are thus attenuated over large thicknesses. Increasing the number of Fourier components to $\pm 100G$ increases the number of Bloch waves to 201 and modifies some of the details of the Bloch-wave branches somewhat. However, propagating modes persist. This observation is consistent with previous reports that waveguide modes can be efficiently excited in subwavelength slit arrays.[8,17–19,27]

The equivalent plots (not shown) for a dielectric grating made from a material with ϵ slightly larger than unity reveal dispersion surfaces that approximate circles with gaps opening up at the intersections of the propagating modes. This is entirely consistent with dispersion plots that are obtained for x rays in crystals. In this limit, transmission anomalies in the zero-order mode can also be strong, and such anomalies are well known in x-ray diffraction from crystals. Evanescent modes also occur, but are usually of little consequence in x-ray diffraction and are ignored.

It is interesting that many Bloch-wave branches in the plots of Fig. 2 intersect other branches, mainly at $k_x=0$ (normal incidence) and $k_x=g/2$ (the Bragg angle). This is particularly true of the evanescent modes. The density of such crossings is highest for the evanescent modes. These crossings are reminiscent of decoupled plane-wave modes in a uniform medium. Further, for the $k_x=0$ normal-incidence conditions studied in depth here, none of these intersecting branches are significantly excited. This suggests that these branches are dynamically decoupled. In dynamical diffraction terms, this means that many of the evanescently diffracted modes have a near-infinite extinction distance at this condition and so do not contribute directly to the scattering.

Figure 2 shows that propagating modes persist out to wavelengths that are significantly longer than the periodicity. Each Bloch wave has its own effective refractive index $n^{(j)}$, given by $n^{(j)}=\lambda k_z^{(j)}/2\pi$. The relative excitation of these Bloch waves is governed entirely by the boundary conditions at the top and bottom surfaces—both surfaces being equally important. It is not just the evanescent Bloch-wave modes

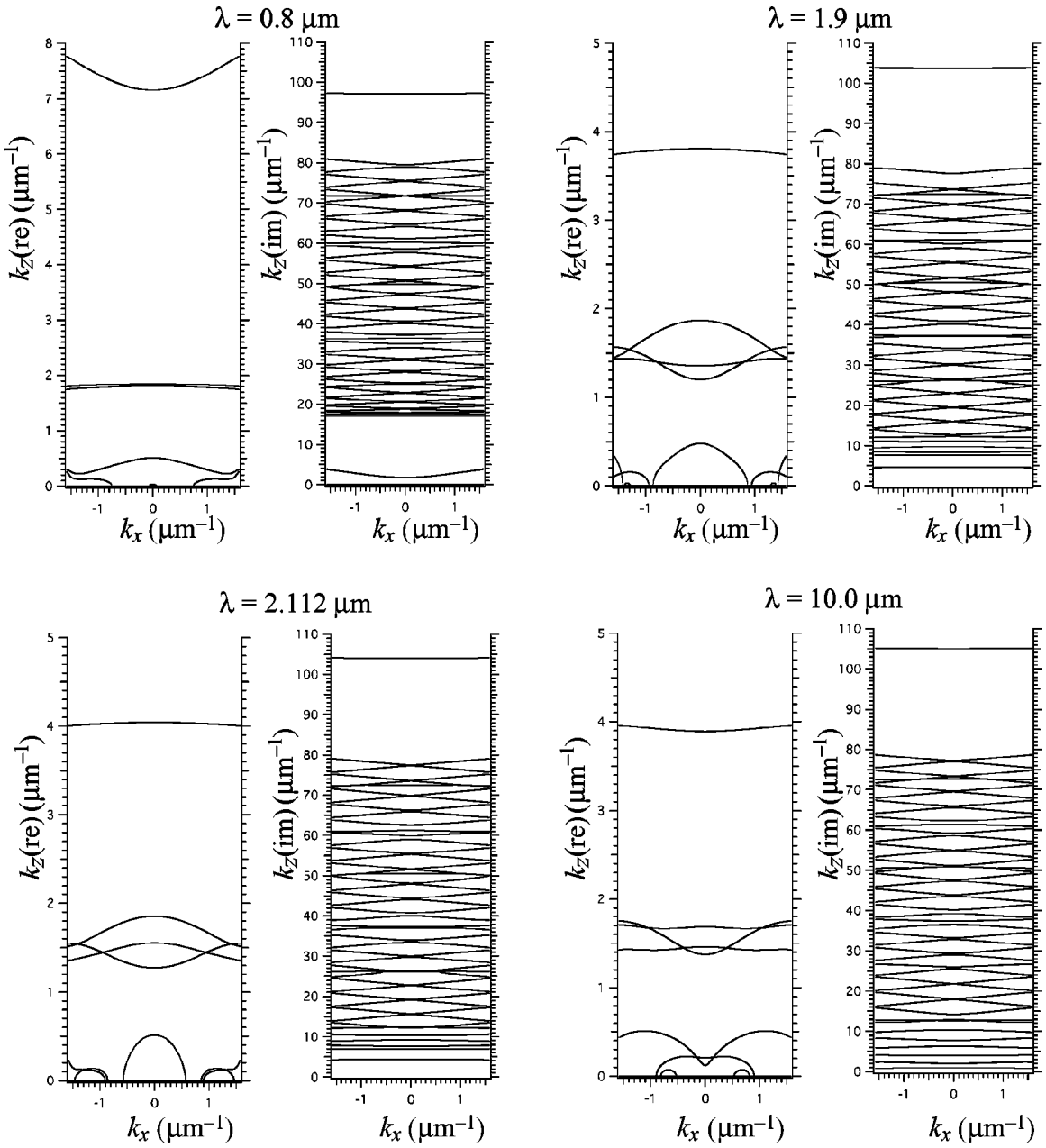

FIG. 2. Plots showing the Bloch-wave dispersion surfaces for four photon wavelengths $\lambda = 0.8$, 1.9, 2.117, and 10.0 μm, respectively. The grating details are the same as for Fig. 1. Each plot shows branches for the propagating Bloch-wave modes (eigenvalue $k_z^{(j)}$ pure real) on the left and for the evanescent modes (eigenvalue $k_z^{(j)}$ pure imaginary) on the right. Note that propagating modes persist at wavelengths much larger than the slit spacing.

(which are most closely associated with the traditional surface plasmons) that are sensitive to the surfaces. *All* modes, including the propagating ones (which are most closely associated with traditional Bragg beams), are dependent on the surfaces. Thus, the observation that the addition of thin silver layers on nickel gratings enhance the transmission[12] does not constitute proof that evanescent modes alone are responsible.

Examination of the Bloch-wave excitations at maximum and minimum transmission reveal that no one mode dominates over all others. It turns out that for maximum transmission in slit arrays (except in the case of negligibly thin films) at least one propagating mode must be strongly excited. In addition, minima corresponding to the Wood-Rayleigh anomalies occur at those conditions where the wave vector $k_z^{(j)}$ of a propagating mode goes to zero. This is a special condition where a mode makes the transition from being a propagating (perhaps attenuated) mode to a purely evanescent mode. Such $k_z^{(j)} = 0$ conditions tend to be strongly resonant.

Figure 3(a) shows the intensity $H^2(\mathbf{r})$ of the total diffracted wave field in the vicinity of the two slits of the grating at $\lambda = 2.117$ μm (100% transmission). Figure 4(a) shows the total intensity at $\lambda = 2.0$ μm (minimum transmission). Figures 3(b)–3(j) and 4(b)–4(j) show the nine dominant

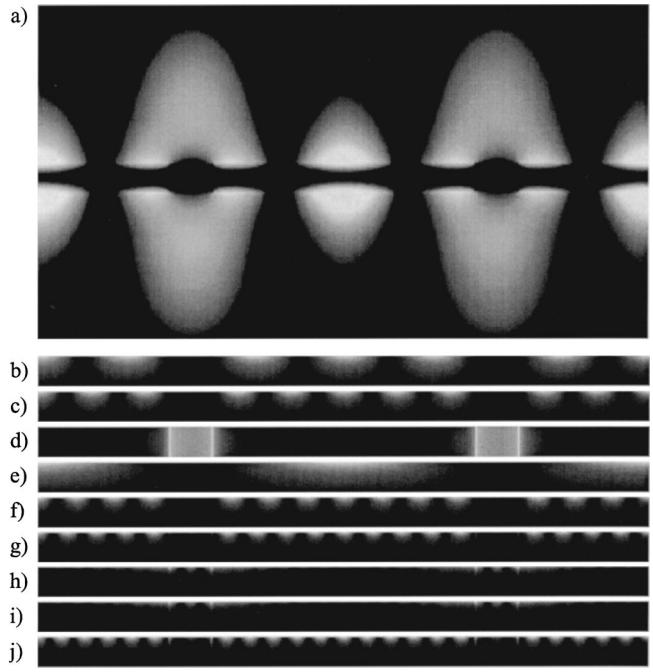

FIG. 3. (a) Side view showing the total photon intensity $H^2(\mathbf{r})$ in the vicinity of the same grating as in Fig. 1 at maximum transmission $\lambda = 2.117\ \mu$m. The simulation was for $\pm 100G$ Fourier components (201 modes total). At maximum (100%) transmission, the intensity distribution is identical at the entrance and exit surfaces. (b)–(j) show the intensities $H^2(\mathbf{r})$ of the nine dominant Bloch-wave modes. Excitations ψ decrease from top to bottom. (b) $|\psi| = 12.557, k_z = 0 + i8.656$; (c) $|\psi| = 0.744, k_z = 0 + i11.317$; (d) $|\psi| = 0.666, k_z = 5.041 + i0$; (e) $|\psi| = 0.478, k_z = 0 + i7.006$; (f) $|\psi| = 0.193, k_z = 0 + i14.466$; (g) $|\psi| = 0.091, k_z = 0 + i17.880$; (h) $|\psi| = 0.086, k_z = -1.858 + i24.917$; (i) $|\psi| = 0.086, k_z = 1.858 + i24.917$; (j) $|\psi| = 0.085, k_z = 0 + i21.589$.

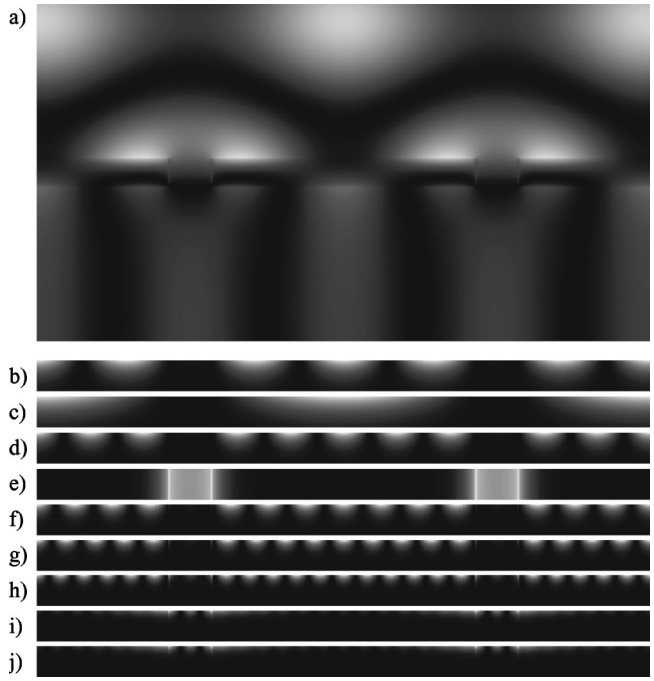

FIG. 4. (a) Side view showing the total photon intensity $H^2(\mathbf{r})$ in the vicinity of the same grating as in Fig. 1 at minimum transmission $\lambda = 2.0\ \mu$m. The simulation was for $\pm 100G$ Fourier components (201 modes total). (b)–(j) show the intensities $H^2(\mathbf{r})$ of the nine dominant Bloch wave modes. Excitations ψ decrease from top to bottom. (b) $|\psi| = 1.999, k_z = 0 + i8.855$; (c) $|\psi| = 1.460, k_z = 0 + i7.247$; (d) $|\psi| = 0.134, k_z = 0 + i11.471$; (e) $|\psi| = 0.121, k_z = -5.172 + i0$; (f) $|\psi| = 0.034, k_z = 0 + i14.587$; (g) $|\psi| = 0.015, k_z = 0 + i17.981$; (h) $|\psi| = 0.014, k_z = 0 + i21.684$; (i) $|\psi| = 0.013, k_z = 1.863 + i24.914$; (j) $|\psi| = 0.013, k_z = -1.863 + i24.914$.

Bloch waves excited in the grating at each condition. Only the modes that decay from (or grow towards[35]) the top surface are shown (wave field 2). A similar set of Bloch waves that decay from the bottom surface (wave field 3) are also excited, but are not shown. Interestingly, at these two extremes, it is essentially the same subset of Bloch waves that dominate. It is primarily the excitation amplitude of each Bloch wave (which is complex) that varies significantly. Note that although the photon intensity near the exit surface at maximum transmission is not ripple free, in the far field the transmitted wave is a plane wave.

Each Bloch-wave mode has a polarization charge density (surface plasmon) associated with it, given by $\rho_{\mathrm{SP}}^{(j)} = -\epsilon_0 \nabla \cdot \mathbf{E}^{(j)}$. This is readily obtained from the **H** form of the Bloch waves via Eq. (11). Not surprisingly, the evanescent Bloch-wave modes correspond to polarization waves that are essentially confined to the upper and lower surfaces of the grating. The propagating mode [Figs. 3(d) and 4(e)] is associated with polarization charge density strongly localized to the walls of the channels, opposite walls being oppositely charged.

Figure 5 shows computed plots for the rocking curves from a Ag grating. In this simulation, the one-dimensional grating has a periodicity of 0.6 μm, slit width of 0.16 μm, and a thickness of 0.2 μm. These plots were computed to match, as far as possible, the experimental conditions of the data published by Ghaemi *et al.* (1998).[2] The plot shows a gray scale representation of the zero-order transmitted intensity as a function of beam tilt (k_x, x axis) and photon energy in eV (z axis). The left-hand side of the plot shows the computation for the unsupported Ag grating. The right-hand side of the plot shows a similar computation for the same grating supported on a quartz plate. Both plots are mirror symmetric about $k_x = 0$, so only half of each plot is shown. The values of ϵ for silver were obtained by a numerical fit to the data of Johnson and Christy,[38]

$$\epsilon_{\mathrm{Ag}} = 4.0 - 54.0\lambda^2 + i\lambda(0.38 + 0.71\lambda^2), \qquad (21)$$

which is valid for the experimental range $0.3\ \mu\mathrm{m} \leqslant \lambda \leqslant 1.94\ \mu$m, but probably can be extrapolated to longer wavelengths without significant loss of precision.

Despite the fact that this is a one-dimensional simulation and the data collected by Ghaemi and co-workers[2] is for a two-dimensional grating, this plot reproduces the essential features of their data remarkably well.

IV. DISCUSSION

In this paper it is demonstrated that the resonance phenomenon that is responsible for the transmission anomalies

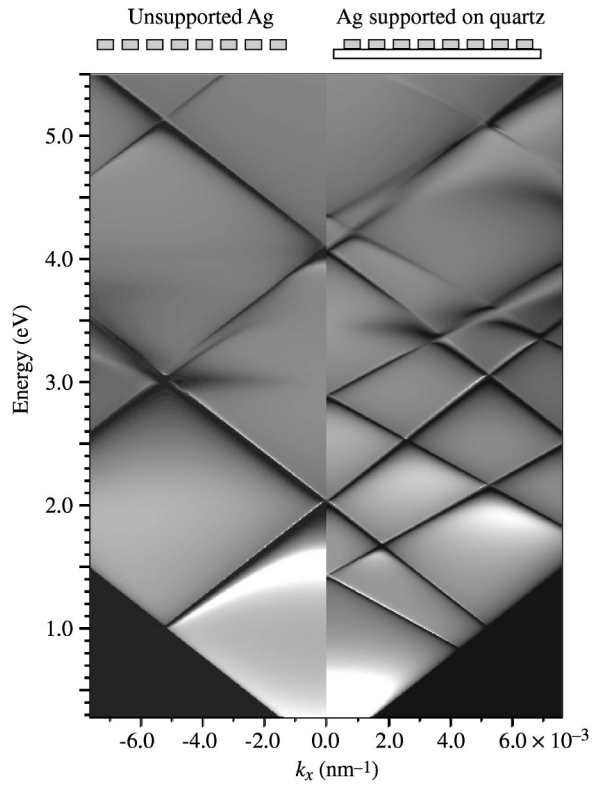

FIG. 5. Computed rocking curves for a one-dimensional Ag grating of periodicity 0.6 μm, slit width 0.16 μm, and thickness of 0.2 μm. The plot shows a gray scale representation of the zero-order transmitted intensity as a function of beam tilt (k_x,x axis) and photon energy in eV (z axis). The left-hand side of the plot shows the computation for the unsupported Ag grating. The right-hand side of the plot shows a similar computation for the same grating supported on a quartz plate ($\epsilon=2$). This plot reproduces many of the features observed in data taken from a two-dimensional Ag hole array (Ref. 2).

in metallic slit arrays is coherent diffraction. Maxwell's equations for the problem can be formulated in terms of a dynamical diffraction Bloch-wave eigensystem, exactly analogous to that presented by Ewald for x-ray diffraction in crystals. Further, this treatment is closely similar to that presented by Meade and co-workers[33,34] for the related study of optical band-gap materials (systems where ϵ is large and positive). It is also shown that surface plasmons are an integral part of the diffracted wave field.

The underlying physics for the metal holes arrays and optical band-gap materials is formally identical. It is only the choice of eigenvalue that differs: wave vector k for this treatment, frequency ω for the band-gap treatment.

The resonance originates in the physical structure of the grating, whose periodicity allows the scattered wave to adopt spatial modes containing the same periodicity. Explanations based on surface plasmons alone appear to miss this point. For example, Martín-Moreno *et al.*[14] (2001) state that "the effect of extraordinary transmission has a resonant nature;" they then admit that "it is not obvious what mechanism is involved." The resonance mechanism is coherent dynamical diffraction. Viewing diffraction modes as Bloch waves, it is found for arrays of slits that while many modes are evanescent (the eigenvalue wave vector $k_z^{(j)}$ is pure imaginary), an important few are propagating or attenuated (the eigenvalue wave vector $k_z^{(j)}$ has a nonzero real part). Propagating modes can persist even when the wavelength is larger than the fundamental array spacing. Surface plasmons arise in all periodic media, and the polarization charge density is given by $-\epsilon_0 \nabla \cdot \mathbf{E}$ in a dielectric medium. Metals, such as silver, are special in that the dielectric permittivity is large and negative, which acts to expel the electric field from the metal. This means that, in metals, the propagating diffraction modes tend to have strong electric fields in the holes.

This statement is consistent with the interpretation of Lalanne and co-workers,[17–19] who point out that the slit cavities can support resonant propagating modes. Essentially, the propagating Bloch-wave modes shown in Figs. 3(d) and 4(e) are the forward-traveling components of such resonant modes. These modes can propagate because there is an effective refractive index n that assures $d<\lambda<nd$. Cao and Lalanne[19] show that a simple model, based on these resonant modes alone, reproduces all the essential features of the full electromagnetic computation. This result illustrates the dominant role played by the propagating Bloch-wave modes (waveguide modes) in slit arrays.

For maximum transmission into the emerging zero-order diffracted beam, the propagating part of the emerging wave field must be a pure plane wave of maximum amplitude. Thus, it is perhaps not so surprising that the transmission maxima tend to occur when $\lambda>d$, the condition where no higher-order propagating diffraction orders can emerge. However, it is not sufficient to excite a single propagating Bloch-wave inside the grating either, since one Bloch wave mode is unlikely to single-handedly match the boundary conditions at the upper and lower surfaces. At maximum and minimum transmission, many modes are excited. For maximum transmission, exact cancellations of the higher-order propagating orders occur, leaving just the $g=0$ order, which carries all the energy out of the grating. Evanescent modes (traditionally associated with surface plasmons) are also excited. For minimum transmission, exact cancellation of the $g=0$ transmitted order occurs and much of the energy is reflected. Surface plasmons are intimately associated with all of the Bloch-wave states, not just the evanescent modes.

It should be pointed out that since all surface plasmon models that have been published to date start by computing the diffracted wave field (**E**,**H**), they too are technically diffraction models. None of these surface plasmon models explicitly contain the plasmon charge density $\rho_{SP}(\mathbf{r})$. In those models, surface plasmons are inferred from the diffracted electric-field distributions. The grating surfaces impose boundary conditions on *all* of the electromagnetic modes that are excited in the grating, including the propagating modes. The surfaces are *not* the exclusive domain of surface plasmons. Since the surface plasmon charge density is given directly by $\rho_{SP}(\mathbf{r})=-\epsilon_0 \nabla \cdot \mathbf{E}$, it is clear that the surface plasmons are in fact an intimate part of the diffracted wave field component **E**. In addition, the physical origin of the resonance, coherent diffraction, is inherently present in these plasmon models. For example, in one study,[15] surface polar-

iton Bloch waves are identified. It is also noted by these authors that intensity enhancements can result from the interference of surface plasmon Bloch waves that have been Bragg scattered by the holes in an array. Technically, being eigenmodes of the photon in the crystal, Bloch waves cannot be further Bragg scattered, since the Bragg scattering of plane-wave states is already folded into the Bloch wave. Nevertheless, theirs is a clear description of dynamical diffraction (multiple scattering).

Several papers[2,9,15] present an expression due to Raether[28] for the wave vector of a surface plasmon on a smooth surface, which is of the type

$$F_0(\mathbf{k}+\mathbf{g})^2=\chi^2. \tag{22}$$

As before, **k** is the photon wave vector, and **g** are the Fourier components of the grating periodicity. F_0 is related to the dielectric permittivities of the metal, ϵ_m, and the holes, ϵ_h, through $F_0=(\epsilon_m+\epsilon_h)/\epsilon_m\epsilon_h$. From this equation for the Ewald sphere, the wave vector of the surface plasmon, k_{SP} is related to the evanescent solutions for k_z, $k_{\mathrm{SP}}=-ik_z$. Equation (22) is one of the diagonal terms of the dynamical scattering matrix, Eq. (14) for the TM polarization. In that case, $F_0=[(d-a)\epsilon_m+a\epsilon_h]/d\epsilon_m\epsilon_h$, the mean value of $1/\epsilon$ in the grating. Equation (22) is correct for a smooth metal surface, with no structural periodicity. However, it ignores the important off-diagonal terms of the dynamical scattering matrix, which describe the coupling between the various scattering modes. As such, Raether's equation is inappropriate for a grating.

Given that the dynamical diffraction model inherently includes surface plasmons, it might reasonably be argued that the issue over whether the transmission anomalies are a diffraction phenomenon or a surface plasmon-enhanced effect is merely a matter of semantics. However, there has been a tendency by proponents of the surface plasmon model to reify surface plasmons by treating them as if they possess independent causal scattering powers. For example, it has been asserted that the metal plays ''an active role'' in enhancing transmission, as opposed to the ''passive'' role of ordinary dielectrics,[1] and it has been declared that surface plasmons actively ''enhance'' transmission[2,9] through metallic hole arrays. It has also been claimed that surface plasmons have the ''found ability'' to ''transmit and focus light very efficiently.''[14] Since the surface plasmons are an integral part of the diffracted wave field, the physical implication, no doubt inadvertent, is that the photon scatters itself or that the surface plasmons pre-exist on the grating.

Polarization waves also occur in ordinary dielectrics, as well as in crystals that are diffracting x rays. The key is that in metallic gratings, the dielectric *response* ϵ tends to be large and negative which influences the phase, amplitude, spatial distribution, and propagation of the polarization waves. Metals are just as passive as ordinary dielectrics.

Although the numerical results presented here are for the simplest case of a one-dimensional grating, which is known to support waveguide modes in the TM polarization mode, the dynamical diffraction equations presented apply fully to gratings that are periodic in three dimensions. For thin gratings, this holds provided the thickness is an integer multiple of repeat units. The dynamical diffraction equation is readily extended to materials in which both $\epsilon(\mathbf{r})$ and $\mu(\mathbf{r})$ vary, although the polarization vectors of each diffracted wave are no longer necessarily perpendicular to the propagation wave vector. No significant departures from the underlying physical interpretation are anticipated by going to higher dimensions. It is clear that the careful study of three-dimensional diffracting geometries, not necessarily periodic or planar, may lead to exciting and useful photonic devices.

ACKNOWLEDGMENTS

I am grateful for numerous discussions with my colleagues, J. Chadi, T. W. Ebbesen, H. F. Ghaemi, R. A. Linke, A. Nahata, T. Thio, L. Wang, and P. A. Wolff, at the NEC Research Institute, Inc., where Ebbesen first reported the anomalous transmission phenomenon. I am also grateful to K. Vepuri for programming assistance.

[1] T. W. Ebbesen, H. J. Lezec, H. F. Ghaemi, T. Thio, and P. A. Wolff, Nature (London) **391**, 667 (1998).
[2] H. F. Ghaemi, T. Thio, D. E. Grupp, T. W. Ebbesen, and H. J. Lezec, Phys. Rev. B **83**, 6779 (1998).
[3] H. A. Bethe, Phys. Rev. **66**, 163 (1944).
[4] P. P. Ewald, Ann. Phys. (Leipzig) **49**, 1 (1916); **49**, 117 (1916).
[5] A. Authier, *Dynamical Theory of X-ray Diffraction* (International Union of Crystallography, Oxford, 2001).
[6] M. M. J. Treacy, Appl. Phys. Lett. **75**, 606 (1999).
[7] U. Schröter and D. Heitmann, Phys. Rev. B **58**, 15 419 (1998).
[8] J. A. Porto, F. J. Garcia-Vidal, and J. B. Pendry, Phys. Rev. Lett. **83**, 2845 (1999).
[9] T. Thio, H. F. Ghaemi, H. J. Lezec, P. A. Wolff, and T. W. Ebbesen, J. Opt. Soc. Am. B **16**, 1743 (1999).
[10] D. E. Grupp, H. J. Lezec, T. Thio, and T. W. Ebbesen, Adv. Mater. **11**, 860 (1999).
[11] T. Thio, H. J. Lezec, and T. W. Ebbesen, Physica B **279**, 90 (2000).
[12] D. E. Grupp, H. J. Lezec, T. W. Ebbesen, K. M. Pellerin, and T. Thio, Appl. Phys. Lett. **77**, 1569 (2000).
[13] C. Sönnichsen, A. C. Duch, G. Steininger, M. Koch, G. von Plessen, and J. Feldman, Appl. Phys. Lett. **76**, 140 (2000).
[14] L. Martín-Moreno, F. J. García-Vidal, H. J. Lezec, K. M. Pellerin, T. Thio, J. B. Pendry, and T. W. Ebbesen, Phys. Rev. Lett. **86**, 1114 (2001).
[15] L. Salomon, F. Grillot, A. V. Zayats, and F. de Fornel, Phys. Rev. Lett. **86**, 1110 (2001).
[16] A. Krishnan, T. Thio, T. J. Kim, H. J. Lezec, T. W. Ebbesen, P. A. Wolfe, J. B. Pendry, L. Martín-Moreno, and F. J. García-Vidal, Opt. Commun. **200**, 1 (2002).
[17] Ph. Lalanne, J. P. Hugonin, S. Astilean, M. Palamaru, and K. D. Möller, J. Opt. A, Pure Appl. Opt. **2**, 48 (2000).

[18] S. Astilean, Ph. Lalanne, and M. Palamaru, Opt. Commun. **175**, 265 (2000).
[19] Q. Cao and P. Lalanne, Phys. Rev. Lett. **88**, 057403 (2002).
[20] R. W. Wood, Philos. Mag. **4**, 396 (1902).
[21] R. M. Wood, Phys. Rev. **48**, 928 (1935).
[22] P. B. Hirsch, A. Howie, R. B. Nicholson, D. W. Pashley, and M. J. Whelan, *Electron Microscopy of Thin Crystals* (Butterworths, Cambridge, MA, 1965).
[23] D. K. Bowen and B. K Tanner, *High Resolution X-ray Diffractometry and Topography* (Taylor & Francis, London, 1998).
[24] M. G. Moharam and T. K. Gaylord, J. Opt. Soc. Am. A **3**, 1780 (1986).
[25] P. Lalanne and G. M. Morris, J. Opt. Soc. Am. A **13**, 779 (1996).
[26] G. Granet and B. Guizal, J. Opt. Soc. Am. A **13**, 1019 (1996).
[27] E. Popov, M. Nevière, S. Enoch, and R. Reinisch, Phys. Rev. B **62**, 16 100 (2000).
[28] H. Raether, *Surface Plasmons on Smooth and Rough Surfaces and on Gratings* (Springer-Verlag, Berlin, 1988).
[29] T. W. Ebbesen, T. Thio, H. F. Ghaemi, and P. A. Wolff, private communications at the NEC Research Institute, Inc., where the anomalous transmission effect was first reported, 1996–2000.
[30] M. Born and E. Wolf, *Principles of Optics* (Pergamon Press, Oxford, 1975).
[31] L. Li, J. Opt. Soc. Am. A **14**, 2758 (1997).
[32] P. Lalanne, Phys. Rev. B **58**, 9801 (1998).
[33] R. D. Meade, A. M. Rappe, K. D. Brommer, J. D. Joannopoulos, and O. L. Alerhand, Phys. Rev. B **48**, 8434 (1993).
[34] J. D. Joannopoulos, R. D. Meade, and J. N. Winn, *Photonic Crystals* (Princeton University Press, Princeton, 1995).
[35] Because of the ambiguity of sign when extracting the k_z from the square root of the eigenvalues, the k_z were chosen so that Bloch-wave modes decay in the $+z$ direction (complex component is always positive). In consequence, some Bloch-wave modes have their real component negative, implying that those modes, when associated with the upper surface, actually propagate in the $-z$ direction. Bloch waves with the opposite sign of k_z are nominally associated with the lower surface and thus redress any imbalance imposed by the arbitrariness of choice of the sign of k_z.
[36] E. Anderson, Z. Bai, C. Bischof, J. Demmel, J. Dongarra, J. Du Croz, A. Greenbaum, S. Hammerling, A. McKenney, S. Ostrouchov, and D. Sorensen, *LAPACK User's Guide*, 2nd ed. (Society for Industrial and Applied Mathematics, Philadelphia, 1995).
[37] L. Li, J. Opt. Soc. Am. A **13**, 1870 (1996).
[38] P. B. Johnson and R. W. Christy, Phys. Rev. B **6**, 4370 (1972).